Preclinical evaluation of thin convex probe endobronchial ultrasound-guided transbronchial needle aspiration for intrapulmonary lesions

Tsukasa Ishiwata[1]^, Terunaga Inage[1], Alexander Gregor[1], Yamato Motooka[1], Harley H. L. Chan[2], Nicholas Bernards[1], Masato Aragaki[1], Zhenchian Chen[1], Hideki Ujiie[1], Tomonari Kinoshita[1], Andrew Effat[1], Kazuhiro Yasufuku[1,2]

[1]Division of Thoracic Surgery, Toronto General Hospital, University Health Network, Toronto, Ontario, Canada; [2]TECHNA Institute for the Advancement of Technology for Health, University Health Network, Toronto, Ontario, Canada

Contributions: (I) Conception and design: T Ishiwata, T Inage, K Yasufuku; (II) Administrative support: K Yasufuku; (III) Provision of study materials or patients: T Ishiwata, T Inage, A Gregor, Y Motooka, N Bernards, M Aragaki, Z Chen, H Ujiie, T Kinoshita, A Effat, K Yasufuku; (IV) Collection and assembly of data: All authors; (V) Data analysis and interpretation: T Ishiwata, T Inage, A Gregor; (VI) Manuscript writing: All authors; (VII) Final approval of manuscript: All authors.

Correspondence to: Kazuhiro Yasufuku, MD, PhD. Head, Division of Thoracic Surgery, University Health Network, William Coco Chair in Surgical Innovation for Lung Cancer, FG Pearson-RJ Ginsberg Chair in Thoracic Surgery, Director of Endoscopy, University Health Network, Director, Interventional Thoracic Surgery Program, University Health Network, Professor, Division of Thoracic Surgery, University of Toronto, Division of Thoracic Surgery, Toronto General Hospital, 200 Elizabeth St, 9N-957, Toronto, ON M5G 2C4, Canada. Email: kazuhiro.yasufuku@uhn.ca.

Background: Conventional flexible bronchoscopy has not achieved the high diagnostic yield for intrapulmonary lesions as seen with image-guided transthoracic biopsy. A thin convex probe endobronchial ultrasound bronchoscope (TCP-EBUS) with a 5.9-mm tip was designed to improve peripheral access over conventional EBUS bronchoscopes to facilitate real-time sampling of intrapulmonary lesions under ultrasound guidance.

Methods: TCP-EBUS was inserted into the distal airways of *ex-vivo* human lungs to assess bronchial accessibility relative to clinically available bronchoscopes. The short- (≤1 h) and medium-term (≤10 d) safety of TCP-EBUS insertion and EBUS-guided transbronchial needle aspiration (TBNA) using a 25-gauge needle were evaluated physiologically and radiologically in live pigs. TCP-EBUS-guided TBNA feasibility was assessed *in-vivo* with pig intrapulmonary pseudo-tumors and *ex-vivo* with resected human lung cancer specimens.

Results: For bronchial accessibility, TCP-EBUS demonstrated greater reach than the 6.6-mm convex probe endobronchial ultrasound (CP-EBUS) in all bronchi, as well as surpassed a 5.5-mm conventional bronchoscope in 63% (131/209) and a 4.8-mm conventional bronchoscope in 27% (57/209) of assessed bronchi. The median bronchial generation and the mean diameter of bronchi TCP-EBUS reached was 4 (range, 3–7) and 3.3±0.7 mm, respectively. No major complications related to TCP-EBUS-guided TBNA in distal airways were observed in the live pigs. Scattered mucosal erythema of the bronchial walls was observed immediately after TCP-EBUS insertion; this self-resolved by day 10. TCP-EBUS could successfully reach and visualize intrapulmonary targets via ultrasound, with no difficulty in needle deployment or sampling.

Conclusions: TCP-EBUS has the potential to facilitate safe real-time transbronchial sampling of intrapulmonary lesions in the central and middle lung fields.

Keywords: Convex probe endobronchial ultrasound (CP-EBUS); endobronchial ultrasound-guided transbronchial needle aspiration (EBUS-TBNA); intrapulmonary lesions; real-time biopsy

^ ORCID: 0000-0003-2369-2698.

Introduction

The detection of abnormal pulmonary lesions has been increasing owing to the widespread use of chest computed-tomography (CT) for lung cancer screening and routine medical care (1,2). For tissue diagnosis of intrapulmonary lesions, CT-guided transthoracic needle aspiration is often performed because of its high diagnostic yield (3). However, transthoracic approaches have non-negligible complication rates (4). Transbronchial biopsy using a flexible bronchoscope (FB) is a much safer procedure (5). The main downside of conventional FB is its low sensitivity for malignant intrapulmonary lesions (6,7). Obtaining adequate tissue from intrapulmonary lesions, especially those located beyond the segmental bronchus, is challenging. The basic principles for accurate transbronchial biopsy of intrapulmonary lesions are: (I) selecting the correct airway to reach the target; (II) approaching the target as close as possible; (III) confirming the location of the target before sampling; and (IV) sampling the same place as confirmed prior (8). For (I), virtual bronchoscopic navigation and electromagnetic navigation guide bronchoscopists to the target lesions. For (II), thin/ultrathin bronchoscopes or robotic bronchoscopes are useful because of their maneuverability. Although fluoroscopy has been used in many institutions for the purpose of (III), radial probe endobronchial ultrasound (RP-EBUS) or cone-beam CT can localize intrapulmonary lesions more precisely. However, it is challenging to achieve (IV) because biopsy tools may shift from the ideal position due to poor instrument stability by the operator or unexpected movement by the patient, including respiratory motion or cough. To overcome these limitations, a 'real-time' modality may be needed, whereby the biopsy instrument is seen during sampling with immediate confirmation of successful target biopsy. Convex probe endobronchial ultrasound (CP-EBUS) guidance may be a good solution. A meta-analysis demonstrated that endobronchial ultrasound-guided transbronchial needle aspiration (EBUS-TBNA) using a conventional CP-EBUS bronchoscope could diagnose malignant intrapulmonary lesions with 91% sensitivity (9). However, a limited number of lung lesions can be visualized by CP-EBUS due to the bronchoscope's limited ability to access bronchi beyond the central lung fields.

A thin convex probe endobronchial ultrasound bronchoscope (TCP-EBUS) bronchoscope was designed to improve access to the periphery over current CP-EBUS bronchoscopes for real-time sampling of intrapulmonary lesions under ultrasound guidance, as we previously reported (10). The purpose of this study was to assess the bronchial accessibility of TCP-EBUS quantitively compared to currently-available conventional bronchoscopes, the safety of TCP-EBUS insertion into the peripheral airways, and the feasibility of TCP-EBUS-guided TBNA of intrapulmonary lesions in the preclinical setting. We present the following article in accordance with the ARRIVE reporting checklist (available at https://tlcr.amegroups.com/article/view/10.21037/tlcr-22-120/rc).

Methods

All animal studies were performed under an animal use protocol (AUP 4150) approved by the Animal Care Committee of the University Health Network (Toronto, Canada), in compliance with national and institutional guidelines for the care and use of animals. Research using human lungs was approved by the Institutional Review Board of the University Health Network (REB #06-0283 approved on May 18, 2006 and REB #16-6083 approved on December 19, 2016), and conducted at Toronto General Hospital (Toronto, Canada) between October 2018 and February 2021. Research consent was obtained in all cases from lung transplantation donors or donors' proxy, and lung cancer patients. This study was conducted in accordance with the amended Declaration of Helsinki (as revised in 2013).

TCP-EBUS

The prototype TCP-EBUS (BF-Y0086, Olympus Medical Systems Corp., Japan) has a distal outer diameter of 5.9 mm with maximum upward flexion of 170 degrees, whereas the conventional CP-EBUS used in this study (BF-Y0063, Olympus Medical Systems Corp.) has a 6.6-mm tip and 160 degrees maximum upward flexion (*Figure 1*). The specifications of the conventional CP-EBUS mirror those found in the commercially available BF-UC190F (Olympus
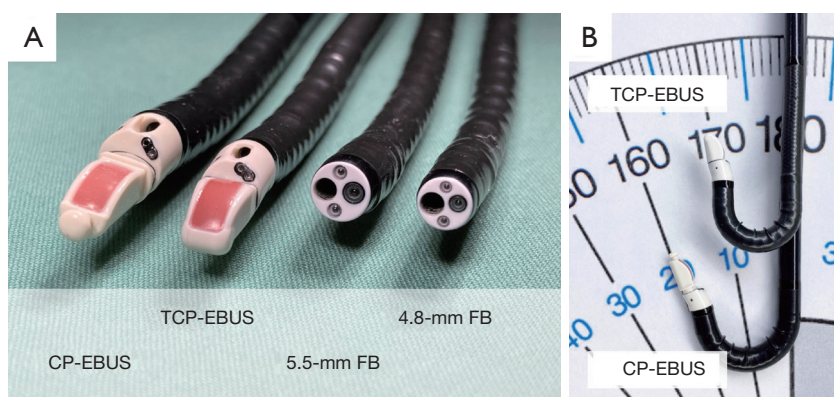
Figure 1 Appearance and specifications of the prototype TCP-EBUS and the conventional bronchoscopes used in this study. (A) The prototype TCP-EBUS (BF-Y0086, Olympus Medical Systems Corp., Japan) has a distal outer diameter of 5.9 mm, angulation range of 170 degrees upward and 70 degrees downward, 14-degree direction of view, and a 1.7-mm working channel inner diameter. TCP-EBUS visualizes a target via direct contact with the bronchial wall, unlike conventional CP-EBUS which uses a saline-filled balloon. For bronchial accessibility assessment, a conventional CP-EBUS (BF-Y0063, Olympus Medical Systems Corp.; this device has the same specifications as the Olympus Medical Systems Corp. BF-UC190F), a 5.5-mm FB (BF-H190, Olympus Medical Systems Corp.), and a 4.8-mm FB (BF-Q190, Olympus Medical Systems Corp.) were used. The conventional CP-EBUS has a 6.6-mm tip, 160-degree upward and 70-degree downward angulation range, and 20-degree direction of view. Both 5.5- and 4.8-mm FBs have a 210-degree upward and 130-degree downward angulation range and 0-degree direction of view. (B) Visual demonstration of the difference in maximum upward angulation between TCP-EBUS and conventional CP-EBUS. TCP-EBUS, thin convex probe endobronchial ultrasound; CP-EBUS, convex probe endobronchial ultrasound; FB, flexible bronchoscope.

Medical Systems Corp.). TCP-EBUS has a 1.7-mm working channel, which can accommodate commercially available 25-gauge EBUS-TBNA needles (NA-U401SX-4025N, Olympus Medical Systems Corp.).

Bronchial accessibility assessment of TCP-EBUS

A total of five *ex-vivo* human lungs declined for lung transplantation within 24 hours after procurement were used to compare the peripheral reach of TCP-EBUS with standard FBs. Since TCP-EBUS had clearly greater reach than a 6.2-mm therapeutic FB (BF-1TH190, Olympus Medical Systems Corp.) and clearly less reach than a 4.2-mm thin FB (BF-P190, Olympus Medical Systems Corp.) in our prior animal experience using live pigs (Figure S1), a 5.5-mm FB (BF-H190, Olympus Medical Systems Corp.) and a 4.8-mm FB (BF-Q190, Olympus Medical Systems Corp.) were used for comparison in this study. *Ex-vivo* human lungs were intubated with an 8.5-mm endotracheal tube and mechanically ventilated with a tidal volume of 7 mL/kg donors' total body weight [mean weight of donor, 79.2 kg; standard deviation (SD), 10.8 kg] with a frequency of 16 per minute. Bronchoscopes were inserted

through the endotracheal tube and the number of bronchial generations passed until the bronchoscope could not be advanced further was counted under direct endoscopic vision. The TCP-EBUS endoscopic camera is off-axis from the bronchoscope tip, which can made endoscopic visualization sometimes difficult. Therefore, the point of maximum TCP-EBUS insertion was physically marked via 25-gauge TBNA needle puncture and then measured by follow-up 2.8-mm ultrathin FB (BF-XP160F, Olympus Medical Systems Corp.) to count the bronchial generations from the trachea to needle mark. Bronchial generation was defined with the main carina counting as generation 1, and subsequent bifurcations resulting in a stepwise increase (e.g., the right upper lobe bronchus, just beyond the second carina, counted as generation 2). Fluoroscopic images were acquired at the point of maximal insertion for all bronchoscopes.

For quantitative assessment of the bronchial diameter that TCP-EBUS can access, an additional three *ex-vivo* human lungs were used. The TCP-EBUS was inserted into the *ex-vivo* human lungs following intubation and ventilation as described above. Once the point of maximal insertion in each bronchopulmonary segment was reached,

a 25-gauge needle was deployed 1 cm into the parenchyma to inject 1 mL of marking gel (mixture of 2% w/w agarose [LS16500100, Thermo Fisher Scientific, MA, USA] and 6% w/w barium sulfate [BA125, Spectrum Chemical MFG, CA, USA]). Cone-beam CT images were acquired after markings with the bronchoscope removed to avoid distortion of the bronchial anatomy during imaging. Acquired CT images were transferred to an image processing program (RadiAnt DICOM viewer version 2020.2.1, Medixant, Poland) to measure the associated feeding bronchi and generate three-dimensional reconstructed images.

Safety assessment of TCP-EBUS-guided TBNA

Male Yorkshire pigs (45±9.1 kg, Caughell Farms Inc., Fingal, Canada) were placed supine, anesthetized with isoflurane, intubated with an 8.5-mm endotracheal tube, and mechanically ventilated with a tidal volume of 7 mL/kg. The TCP-EBUS was advanced until significant resistance was encountered; at this point, a fluoroscopic image was acquired to document the TCP-EBUS position. EBUS-TBNA in the peripheral lungs was performed five times at the same location with ten agitations of a 25-gauge needle using fluoroscopy. Procedures were performed by a different bronchoscopist for each pig. The TCP-EBUS was then removed and a 2.8-mm ultrathin FB (BF-XP160F, Olympus Medical Systems Corp.) was inserted to document endobronchial findings post-EBUS-TBNA.

To evaluate short-term safety, TCP-EBUS-guided TBNA in the lung periphery was performed in a pig followed by continuous vital sign and clinical monitoring for 1 hour post-procedure. To assess medium-term safety, a total of four pigs were used. Their overall veterinary health was monitored daily for up to 10 days after TCP-EBUS-guided TBNA. On day 10, cone-beam CT of the lungs were acquired and endobronchial findings were captured by ultrathin FB (BF-XP160F). In both settings, at the end of the observation period, the chest wall was surgically opened and the lungs resected. Pigs were sacrificed by potassium chloride injection immediately prior to lung excision. The bronchi where TCP-EBUS was inserted were incised longitudinally *ex-vivo* for gross pathological evaluation.

Feasibility assessment of TCP-EBUS-guided TBNA

To initially assess the feasibility of TCP-EBUS-guided TBNA, an intrapulmonary pseudo-tumor porcine model was used in six pigs. Pseudo-tumors were composed of

agarose (2% w/w; LS16500100, Thermo Fisher Scientific), barium sulfate (6% w/w; BA125, Spectrum Chemical MFG), and methylene blue (MET201, BioShop, ON, Canada) as a blue dye, dissolved together in sterile water. A thin bronchoscope (BF-P190) was advanced to the 4th generation bronchus and a 21-gauge needle (NA-403D-2021, Olympus Medical Systems Corp.) was deployed to inject 3 mL of pseudo-tumor mixture into the lung parenchyma. After the creation of the lung pseudo-tumor, the TCP-EBUS was inserted into the peripheral airway to localize the pseudo-tumor followed by EBUS-TBNA. Successful tissue collection of the pseudo-tumor was defined as acquiring blue-colored specimens. In addition to the intrapulmonary pseudo-tumors, mediastinal lymph nodes (subcarinal and lower paratracheal nodes) were approached by TCP-EBUS and EBUS-TBNA was performed. All EBUS-TBNA procedures were performed with a 25-gauge needle.

To confirm the feasibility of TCP-EBUS-guided TBNA for human lung cancers, three resected human lung cancer specimens were used. Patients who had a preoperative diagnosis of lung cancer and were scheduled to undergo lobectomy or pneumonectomy were screened, and patients with lung tumors situated in the middle-third lung field were selected. Within 10 mins after lung resection, the specimen's stapled bronchial stump was opened *ex-vivo* and the TCP-EBUS inserted to localize the lung cancer. After visualization of the target, a 25-gauge needle was deployed through the working channel and EBUS-TBNA was performed with 20 mL of vacuum. The aspirated specimen was smeared onto glass slides. Air-dried smears were stained using a modified Giemsa stain (Diff-Quik, American Scientific Product, IL, USA) for cytological evaluation. Successful sampling was defined as confirmation of malignant cells by a cytopathologist.

Statistical analysis

Given the small number of subjects assessed in this preclinical study, only descriptive analysis was appropriate. Summary statistics were calculated using GraphPad Prism 8 (GraphPad Software, CA, USA). Continuous variables were summarized as either median with range or mean with SD.

Results

A total of 209 bronchi in five *ex-vivo* human lungs were used for bronchial accessibility comparison; bronchial generation
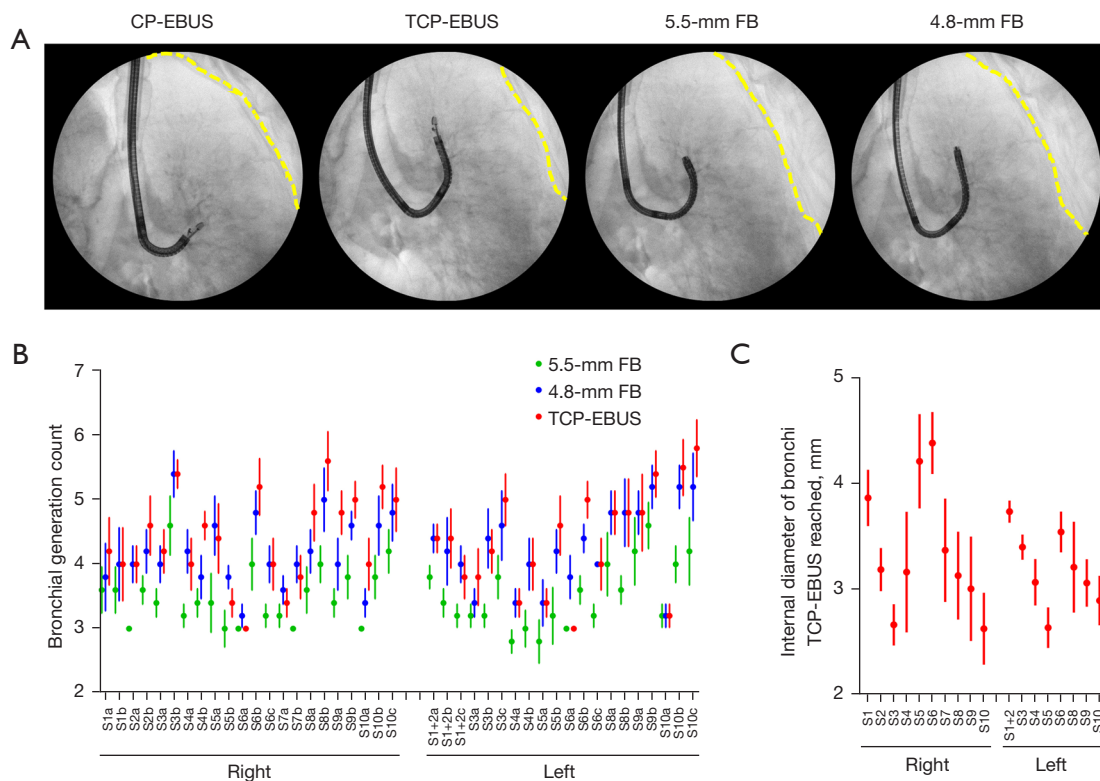
Figure 2 Bronchial accessibility of TCP-EBUS in distal airways. (A) Representative fluoroscopic images of each bronchoscope inserted into left $B^{1+2}a$ of an *ex-vivo* human lung. Yellow dashed line represents the lateral edge of the lung. (B) Bronchial generation reached at the point of maximal insertion for each bronchoscope (green, 5.5-mm FB; blue, 4.8-mm FB; red, TCP-EBUS), stratified by attempted subsegment in *ex-vivo* human lungs. Dots and bars show the mean and SD. Not all bronchoscopes were ultimately able to access the corresponding subsegmental bronchus due to size or flexibility limitations. (C) Mean diameter of bronchi TCP-EBUS reached, measured by CT, computed tomography scan following barium marking in *ex-vivo* human lungs. The overall average diameter was 3.3 mm (SD 0.7 mm). Red dots and bars show the mean and SD. CP-EBUS, convex probe endobronchial ultrasound; TCP-EBUS, thin convex probe endobronchial ultrasound; FB, flexible bronchoscope; SD, standard deviation.

was not assessed in one bronchus due to inability to identify the needle puncture site. TCP-EBUS demonstrated greater reach than conventional CP-EBUS in all bronchi, as well as surpassed the 5.5-mm FB in 63% (131/209), and the 4.8-mm FB in 27% (57/209) of bronchi (*Figure 2A*, Figure S2). The median bronchial generation reached by TCP-EBUS was 4 (range, 3–7) (*Figure 2B*). The mean diameter of bronchi TCP-EBUS reached was 3.3 mm (SD 0.7 mm) (*Figure 2C*), as measured by CT scan following barium marking. These depth markings largely fell within the middle-third lung field (*Video 1*).

No major complications related to TCP-EBUS insertion into peripheral airways nor performing EBUS-TBNA in the periphery were noted. Scattered mucosal erythema of the bronchial walls was seen immediately after TCP-EBUS

insertion in all pigs; however, this self-resolved by day 10 (*Figure 3*, Figure S3). No active bleeding nor laceration of the bronchial mucosa were observed after TCP-EBUS insertion. All pigs showed normal respiratory status over the 10-day monitoring period. No significant abnormalities were seen on lung CT on day 10 (Figure S4).

Fluoroscopic images showed little restriction in upward-angulation of the TCP-EBUS when a 25-gauge needle was deployed, even in the apical peripheral airways of *ex-vivo* human lungs (*Figure 4A*). In the porcine pseudo-tumor models, TCP-EBUS could successfully reach all targets and visualize them clearly on ultrasound, with no difficulty in needle deployment or sampling with a 25-gauge needle (*Figure 4B-4E*). There were no complications *in-vivo*. Lymph node sampling by TCP-EBUS with a

25-gauge needle was also successful without impaired visualization for all eighteen evaluated lymph nodes (subcarinal and lower paratracheal lymph nodes) (Figure S5).
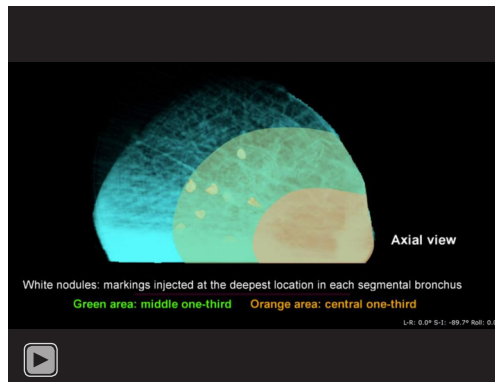

Video 1 Three-dimensional reconstructed CT images of an *ex-vivo* right lower human lung following marking at the point of maximum thin convex probe endobronchial ultrasound insertion.

In the resected human lung cancer specimens, all tumors located in the middle-third lung fields were transbronchially accessible by TCP-EBUS and successfully sampled with a 25-gauge needle under real-time ultrasound guidance (*Figure 4F-4H*). The cytological diagnosis from TCP-EBUS sampling was concordant with the final pathological diagnosis in all cases (Table S1).

Discussion

The present study demonstrated that TCP-EBUS could reliably and safely access the inner two-thirds lung fields for biopsy of intrapulmonary lesions under real-time ultrasound guidance.

Radiographic analysis in our study showed that TCP-EBUS reliably accesses the middle-third lung fields. The reach of TCP-EBUS into the periphery was significantly better than the conventional 6.6-mm CP-EBUS and a 5.5-mm FB, as well as nearly equal to that of a 4.8-mm
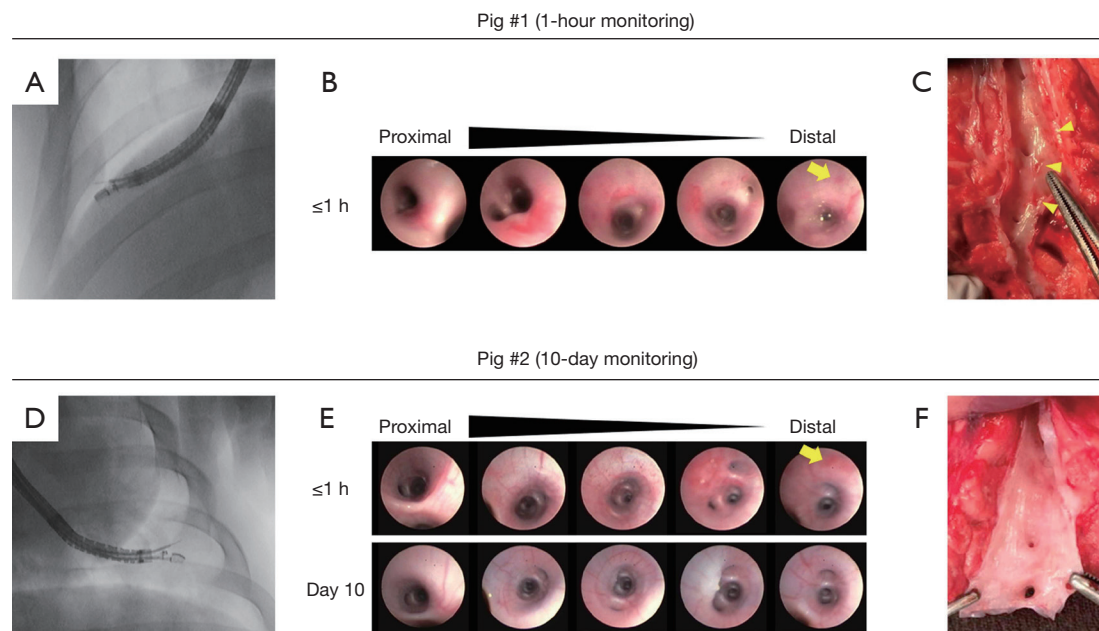
Figure 3 TCP-EBUS-guided TBNA in the peripheral lungs of live pigs. Top: the short-term (≤1 h) safety in pig #1, bottom: the medium-term (10 days) safety in a representative case (pig #2). TCP-EBUS was inserted and EBUS-guided TBNA was performed in the right lower lobe in pig #1 (A) and the left lower lobe in pig #2 (D). Scattered mucosal erythema of the bronchial walls was seen on bronchoscopy within one hour after TCP-EBUS-guided TBNA in the peripheral lung (B,E; yellow arrows indicate the needle insertion point), which was also confirmed on gross pathology (C, yellow arrow heads showing scattered erythema). No active bleeding nor laceration of the bronchial mucosa was observed after TCP-EBUS insertion. The mucosal erythema self-resolved by day 10 (E,F). Pigs showed normal respiratory status over the 10-day monitoring period. TCP-EBUS, thin convex probe endobronchial ultrasound; TBNA, transbronchial needle aspiration.
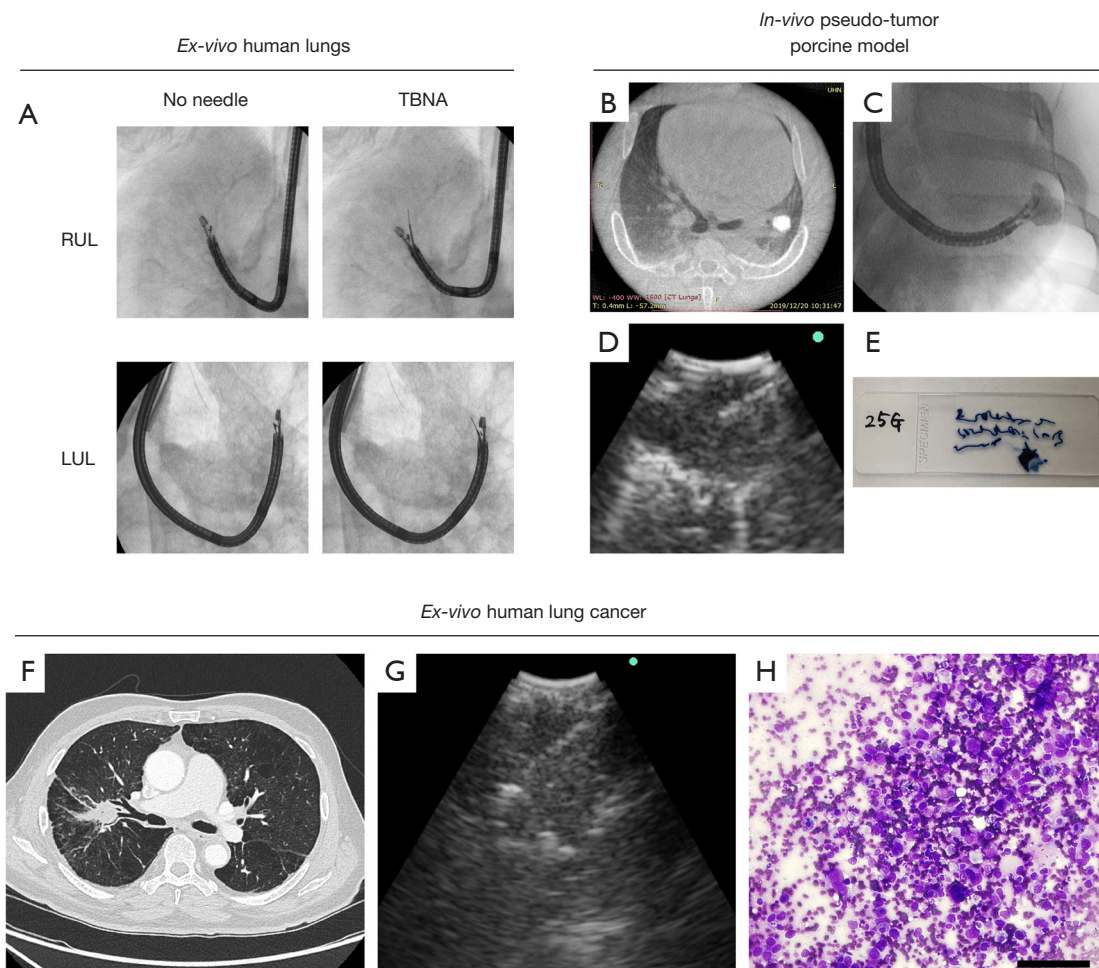
Figure 4 Feasibility assessment of TCP-EBUS-guided TBNA. (A) Representative fluoroscopic images of the *ex-vivo* human lung apices demonstrate that upward angulation of TCP-EBUS is not significantly impacted by 25-gauge TBNA needle insertion or deployment in the distal airways. (B) TCP-EBUS-guided TBNA was performed in *in-vivo* pseudo-tumor porcine models. An axial CT image of a representative pseudo-tumor created in the left upper lobe is shown. The deployed 25-gauge TBNA needle is clearly seen on both (C) fluoroscopic and (D) ultrasound images. (E) Successful sampling of the pseudo-tumor is confirmed by the biopsy specimen's blue color. (F) TCP-EBUS-guided TBNA was successfully performed in a resected human lung cancer specimen. In a representative case, a 35 mm tumor was in the middle-third lung field. The TCP-EBUS was inserted into the resected right upper lobe to approach the target. (G) A 25-gauge TBNA needle deployed through the TCP-EBUS working channel is clearly seen on ultrasound. (H) The acquired sample demonstrated adenocarcinoma using a modified Giemsa stain (scale bar, 200 µm). All TCP-EBUS-guided TBNA were performed without any complications *in-vivo*. TCP-EBUS, thin convex probe endobronchial ultrasound; TBNA, transbronchial needle aspiration; CT, computed tomography; RUL, right upper lobe; LUL, left upper lobe.

FB. This is despite TCP-EBUS having a 5.9-mm distal tip diameter. This performance relative to the 5.5-mm FB may be attributed to the shape of the TCP-EBUS tip, which is more tapered than the flat tip in conventional bronchoscopes. The tapered tip may avoid getting stuck at the bifurcations of peripheral bronchi. The flexibility of TCP-EBUS was also shown, especially in accessing the apices. Flexion was not limited by the presence of a 25-gauge needle in the working channel, and the needle could be inserted and removed repeatedly while maintaining TCP-EBUS position in the peripheral airway. TCP-EBUS may therefore not need to be pulled back to the central

airway for each needle insertion through the working channel when repeating biopsies. In addition to reducing the need to re-localize the target for each biopsy pass, this position stability may also allow tamponade of the inserted bronchus in the event of biopsy-related bleeding. Notably, no biopsy-related bleeding was observed in this study.

Since TCP-EBUS went further than smaller conventional bronchoscopes, one concern was potential mucosal injury secondary to overdilation of the peripheral airways during insertion. Our results suggest this concern remains only hypothetical. No active bleeding nor laceration of the bronchial mucosa was observed. Only minimal, self-resolving mucosal erythema was seen over the 10-day monitoring period. One of the main advantages of TCP-EBUS-guided TBNA for intrapulmonary lesions is a potentially safer profile compared to conventional transbronchial sampling; real-time ultrasound guidance permitted continuous confirmation of needle tip position with regards to depth and relation to vessels. Doppler ultrasound assessment may reduce the risk of hemorrhage and improve the quality of the specimen by avoiding vessels crossing within the target as well.

Real-time ultrasound may be essential for improving the diagnostic yield for transbronchial biopsy of intrapulmonary lesions. The impact of ultrasound guidance on biopsy success is best demonstrated by the high sensitivity and specificity of EBUS-TBNA for lymph node staging (11). Admittedly, TCP-EBUS has less peripheral reach than current thin and ultrathin bronchoscopes. A prospective multicenter study showed that ultrathin bronchoscopes were able to reach the median 5th generation and maximum 9th generation bronchi (12). However, this improved reach does not translate necessarily into high diagnostic yield, reaching only 70.0% (95% CI: 65.0–75.1%) in one meta-analysis (13). The integration of non-real-time ultrasound similarly does not seem sufficient. In a previous prospective multicenter study, a 3.0-mm ultrathin bronchoscope was used in combination with RP-EBUS for diagnosis of peripheral lesions (median diameter 19.0 mm) (14). Although 95% of lesions were successfully visualized by RP-EBUS (concentric and eccentric views), the diagnostic yield was just 74%. With RP-EBUS, there is no assurance that the biopsy instrument can successfully obtain tissue as the radial probe is withdrawn following identification of the target lesion. This is especially true for lung lesions appearing eccentric on RP-EBUS, where even if instrument position is kept perfectly stable, the biopsy instrument may sample in a different direction away from the target.

This would fit with the data showing significantly lower diagnostic yield when the RP-EBUS probe was adjacent to the lesion (i.e., eccentric view) compared to when the probe was within it (i.e., concentric view) (15,16). The integration of ultrasound as a real-time modality is likely key to dramatically improving the yield of transbronchial biopsy. TCP-EBUS can maintain visualization of the target from localization through biopsy, even for peribronchial lesions that would otherwise be 'eccentric' on RP-EBUS.

An attractive potential benefit of TCP-EBUS is that biopsies from mediastinal lymph nodes and intrapulmonary lesions can be performed in a single examination. Staging guidelines for lung cancer recommend mediastinal nodal staging by EBUS-TBNA in patients with suspected or proven non-small cell lung cancer in the presence of (I) abnormal mediastinal/hilar nodes on CT or fluorodeoxyglucose-positron emission tomography; (II) tumor size of >3 cm; or (III) centrally located tumors (17). If the patient has indications for mediastinal staging and has a tumor accessible by TCP-EBUS, consolidating nodal staging and primary tumor biopsy into a single procedure may reduce burdens on patients and the medical system.

Despite our promising results, there is currently no data on the safety, accessibility, and diagnostic yield of TCP-EBUS in the clinical setting, and thus our ability to compare its performance with 'gold-standard' transthoracic biopsy is limited. Nonetheless, we hypothesize that TCP-EBUS may be preferable to transthoracic biopsy for lesions located within the inner two-thirds lung fields by virtue of limiting the parenchymal puncture length and enabling simultaneous diagnosis-and-staging (with the logistical/cost benefits this may entail). Such assessment is planned for a future clinical study.

One possible drawback of TCP-EBUS would be its forward oblique direction of view. Although this angle is less than that of conventional CP-EBUS (14 *vs.* 20 degrees), the oblique direction of view may complicate identification and entry into airway branches under direct vision, especially small airways. Our study demonstrated the potential accessibility of TCP-EBUS into the periphery was promising. However, the ability to select the appropriate airway branch by bronchoscopic view remains to be assessed.

There are some limitations in this study. First, a limited number of *ex-vivo* human lungs were used to assess TCP-EBUS bronchial accessibility, and thus the full variability in lung size and anatomy may not have been effectively captured. Moreover, the *ex-vivo* human lungs were not fixed in the rib cage during assessment. This might bias

our evaluation of bronchial accessibility. The chest wall inherently restricts lung inflation, and thus bronchi may be narrower *in-vivo* than when evaluated *ex-vivo*. Conversely, the relative fixation of the lung within the rib cage may discourage curve/loop formation of the bronchoscope and thus facilitate deeper insertion. Performing *ex-vivo* lung assessment without the chest wall could therefore both over- and underestimate bronchial accessibility depending on the lung region. For example, lower lung zones may benefit more from the greater bronchial diameter of *ex-vivo* assessment, while apical lung zones may benefit more from the relative lung fixation that would be available with *in-vivo* assessment. The *ex-vivo* data must therefore be viewed as strongly predictive, but not definitive, on the potential clinical utility of TCP-EBUS. Second, the number of resected human lung cancer specimens assessed in this study was limited. The use of resected human lung cancer specimens, rather than *in-vivo* assessment, means the diagnostic yield of TCP-EBUS-guided TBNA for human lung cancer cannot be definitively concluded from this study alone; a formal clinical study is required. Third, the pig pseudo-tumors and resected human lung cancers in this study were located adjacent to the bronchus, and no lesions were >5 mm away from the bronchus. Whether TCP-EBUS remains effective at greater distances from the bronchus remains to be seen. We plan to characterize TCP-EBUS ultrasound visualization of lesions without a bronchus sign using *ex-vivo* resected human lung cancer specimens in a future study.

Conclusions

This preclinical study demonstrates that TCP-EBUS can safely access the inner two-thirds lung fields for biopsy of intrapulmonary lesions under real-time ultrasound guidance. This new approach to intrapulmonary lesions may improve the diagnostic yield of transbronchial biopsy while maintaining its safety profile. Further clinical evaluation is needed to more definitively conclude on TCP-EBUS' performance and potential impact on current practice.

Acknowledgments

Footnote

Reporting Checklist: The authors have completed the ARRIVE reporting checklist. Available at https://tlcr.amegroups.com/article/view/10.21037/tlcr-22-120/rc

Data Sharing Statement: Available at https://tlcr.amegroups.com/article/view/10.21037/tlcr-22-120/dss

Conflicts of Interest: All authors have completed the ICMJE uniform disclosure form (available at https://tlcr.amegroups.com/article/view/10.21037/tlcr-22-120/coif). KY reports support from the William Coco Chair in Surgical Innovation for Lung Cancer, during the conduct of this study; KY is a consultant for Olympus Medical Systems Corporation. The other authors have no conflicts of interest to declare.

Ethical Statement: The authors are accountable for all aspects of the work in ensuring that questions related to the accuracy or integrity of any part of the work are appropriately investigated and resolved. Research using human lungs was approved by the Institutional Review Board of the University Health Network (REB #06-0283 approved on May 18, 2006 and REB #16-6083 approved on December 19, 2016), and conducted at Toronto General Hospital (Toronto, Canada) between October 2018 and February 2021. Research consent was obtained in all cases from lung transplantation donors or donors' proxy, and lung cancer patients. This study was conducted in accordance with the amended Declaration of Helsinki (as revised in 2013). All animal studies were performed under an animal use protocol (AUP 4150) approved by the Animal Care Committee of the University Health Network (Toronto, Canada), in compliance with national and institutional guidelines for the care and use of animals.

Open Access Statement: This is an Open Access article distributed in accordance with the Creative Commons Attribution-NonCommercial-NoDerivs 4.0 International License (CC BY-NC-ND 4.0), which permits the non-commercial replication and distribution of the article with the strict proviso that no changes or edits are made and the original work is properly cited (including links to both the

formal publication through the relevant DOI and the license). See: https://creativecommons.org/licenses/by-nc-nd/4.0/.

References

1. National Lung Screening Trial Research Team; Aberle DR, Adams AM, et al. Reduced lung-cancer mortality with low-dose computed tomographic screening. N Engl J Med 2011;365:395-409.
2. Gould MK, Tang T, Liu IL, et al. Recent Trends in the Identification of Incidental Pulmonary Nodules. Am J Respir Crit Care Med 2015;192:1208-14.
3. DiBardino DM, Yarmus LB, Semaan RW. Transthoracic needle biopsy of the lung. J Thorac Dis 2015;7:S304-16.
4. Heerink WJ, de Bock GH, de Jonge GJ, et al. Complication rates of CT-guided transthoracic lung biopsy: meta-analysis. Eur Radiol 2017;27:138-48.
5. Asano F, Aoe M, Ohsaki Y, et al. Deaths and complications associated with respiratory endoscopy: a survey by the Japan Society for Respiratory Endoscopy in 2010. Respirology 2012;17:478-85.
6. Rivera MP, Mehta AC, Wahidi MM. Establishing the diagnosis of lung cancer: Diagnosis and management of lung cancer, 3rd ed: American College of Chest Physicians evidence-based clinical practice guidelines. Chest 2013;143:e142S-65S.
7. Ost DE, Ernst A, Lei X, et al. Diagnostic Yield and Complications of Bronchoscopy for Peripheral Lung Lesions. Results of the AQuIRE Registry. Am J Respir Crit Care Med 2016;193:68-77.
8. Ishiwata T, Gregor A, Inage T, et al. Advances in interventional diagnostic bronchoscopy for peripheral pulmonary lesions. Expert Rev Respir Med 2019;13:885-97.
9. Kuijvenhoven JC, Leoncini F, Crombag LC, et al. Endobronchial Ultrasound for the Diagnosis of Centrally Located Lung Tumors: A Systematic Review and Meta-Analysis. Respiration 2020;99:441-50.
10. Wada H, Hirohashi K, Nakajima T, et al. Assessment of the new thin convex probe endobronchial ultrasound bronchoscope and the dedicated aspiration needle: a preliminary study in the porcine lung. J Bronchology Interv Pulmonol 2015;22:20-7.
11. Silvestri GA, Gonzalez AV, Jantz MA, et al. Methods for staging non-small cell lung cancer: Diagnosis and management of lung cancer, 3rd ed: American College of Chest Physicians evidence-based clinical practice guidelines. Chest 2013;143:e211S-50S.
12. Asano F, Shinagawa N, Ishida T, et al. Virtual bronchoscopic navigation combined with ultrathin bronchoscopy. A randomized clinical trial. Am J Respir Crit Care Med 2013;188:327-33.
13. Wang Memoli JS, Nietert PJ, Silvestri GA. Meta-analysis of guided bronchoscopy for the evaluation of the pulmonary nodule. Chest 2012;142:385-93.
14. Oki M, Saka H, Ando M, et al. Ultrathin Bronchoscopy with Multimodal Devices for Peripheral Pulmonary Lesions. A Randomized Trial. Am J Respir Crit Care Med 2015;192:468-76.
15. Kurimoto N, Miyazawa T, Okimasa S, et al. Endobronchial ultrasonography using a guide sheath increases the ability to diagnose peripheral pulmonary lesions endoscopically. Chest 2004;126:959-65.
16. Yamada N, Yamazaki K, Kurimoto N, et al. Factors related to diagnostic yield of transbronchial biopsy using endobronchial ultrasonography with a guide sheath in small peripheral pulmonary lesions. Chest 2007;132:603-8.
17. Vilmann P, Clementsen PF, Colella S, et al. Combined endobronchial and oesophageal endosonography for the diagnosis and staging of lung cancer. European Society of Gastrointestinal Endoscopy (ESGE) Guideline, in cooperation with the European Respiratory Society (ERS) and the European Society of Thoracic Surgeons (ESTS). Eur Respir J 2015;46:40-60.
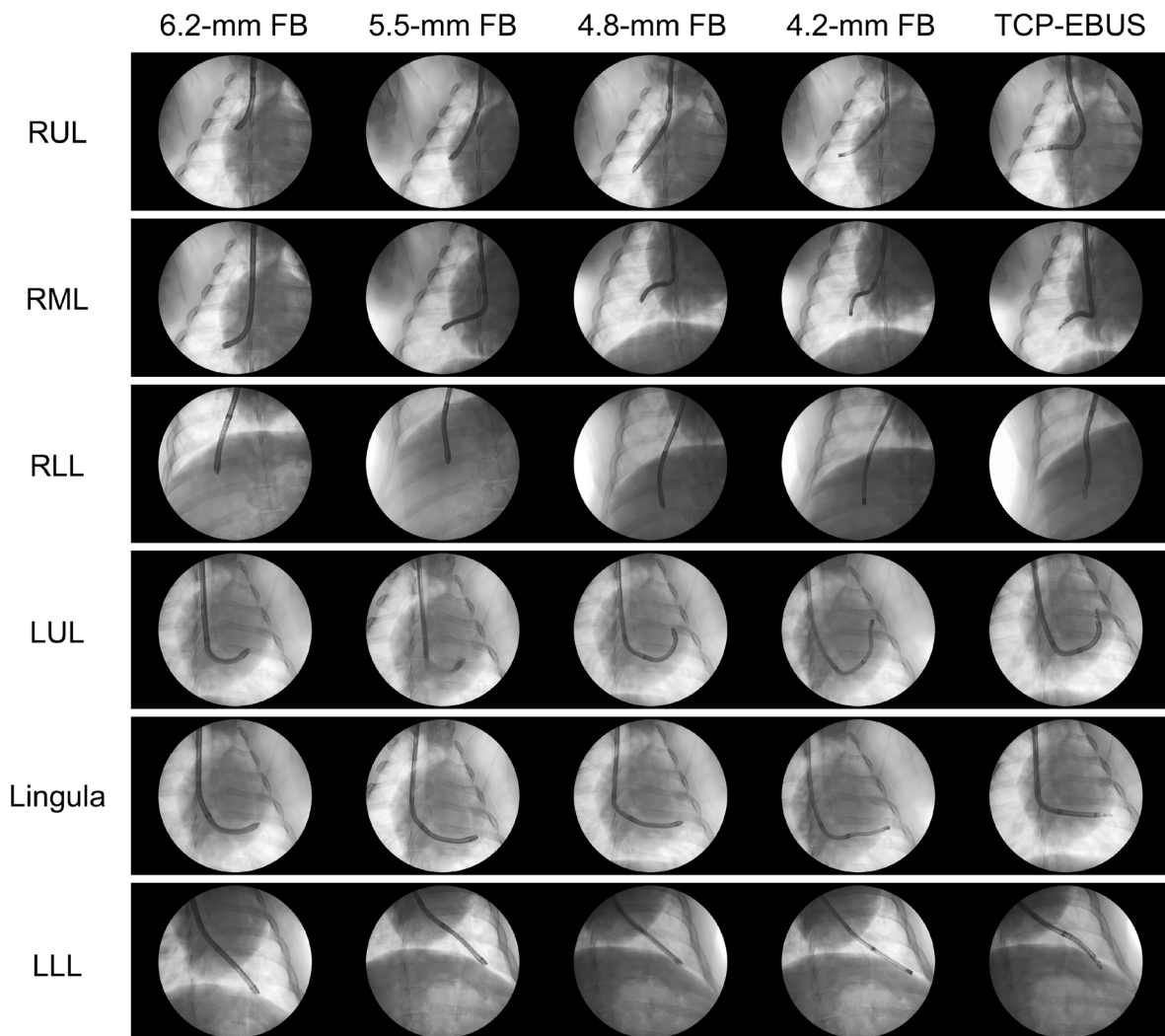
Figure S1 Preliminary radiological assessment of TCP-EBUS peripheral reach using *in-vivo* pig lungs. TCP-EBUS was compared with clinically available FBs including a 6.2-mm therapeutic FB (BF-1TH190), a 5.5-mm FB (BF-H190), a 4.8-mm FB (BF-Q190), and a 4.2-mm FB (BF-P190) (all bronchoscopes from Olympus Medical Systems Corp., Japan). Bronchoscopes were inserted through an 8.5-mm endotracheal tube without fluoroscopy until significant resistance was encountered; at this point, a fluoroscopic image documented the bronchoscope position. TCP-EBUS went obviously further than the 6.2-mm FB and less far than the 4.2-mm FB. Based on these results, TCP-EBUS was compared more comprehensively with the 5.5-mm and 4.8-mm FBs in the current study. TCP-EBUS, thin convex probe endobronchial ultrasound; FB, flexible bronchoscope, RUL, right upper lobe; RML, right middle lobe; RLL, right lower lobe; LUL, left upper lobe; LLL, left lower lobe.
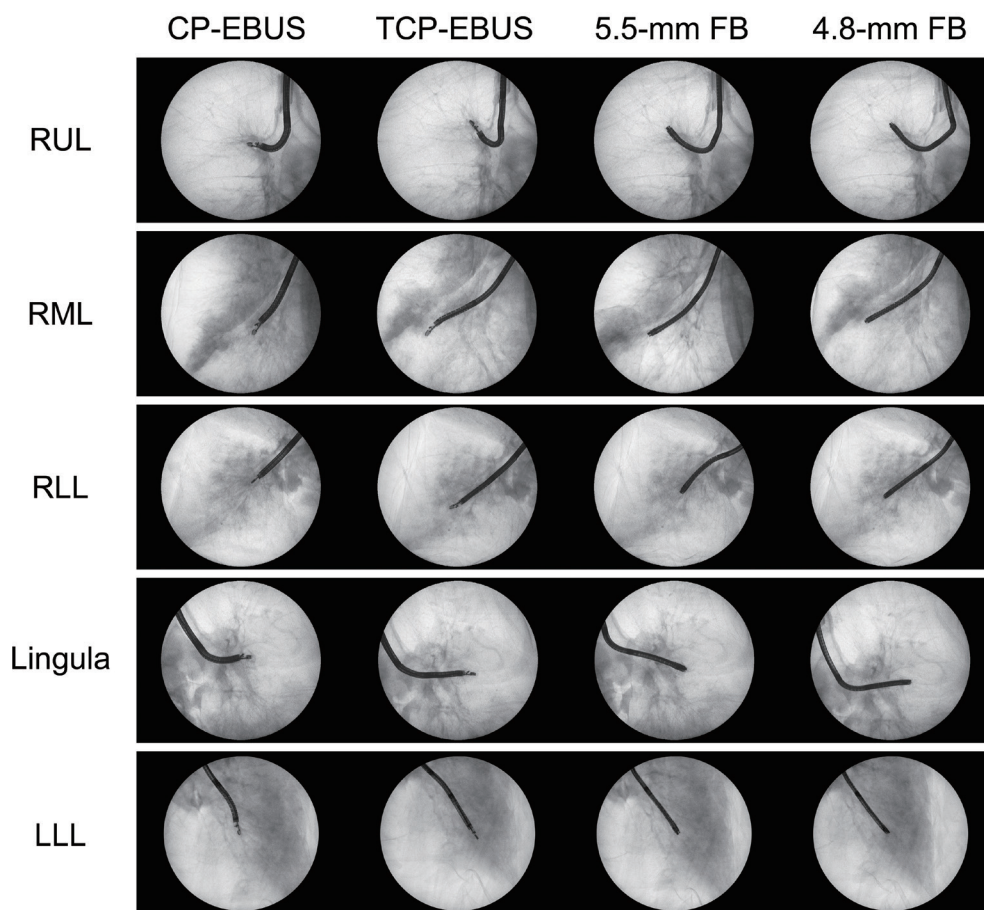
Figure S2 Additional representative fluoroscopic images of TCP-EBUS insertion into the distal airways of ex-vivo human lungs. Bronchoscopes were inserted into the right upper lobe (RUL, rtB^{1}b), right middle lobe (RML, rtB^{4}b), right lower lobe (RLL, rtB^{9}b), lingula (ltB^{4}a), left lower lobe (LLL, ltB^{9}b). CP-EBUS, convex probe endobronchial ultrasound; TCP-EBUS, thin convex probe endobronchial ultrasound; FB, flexible bronchoscope.
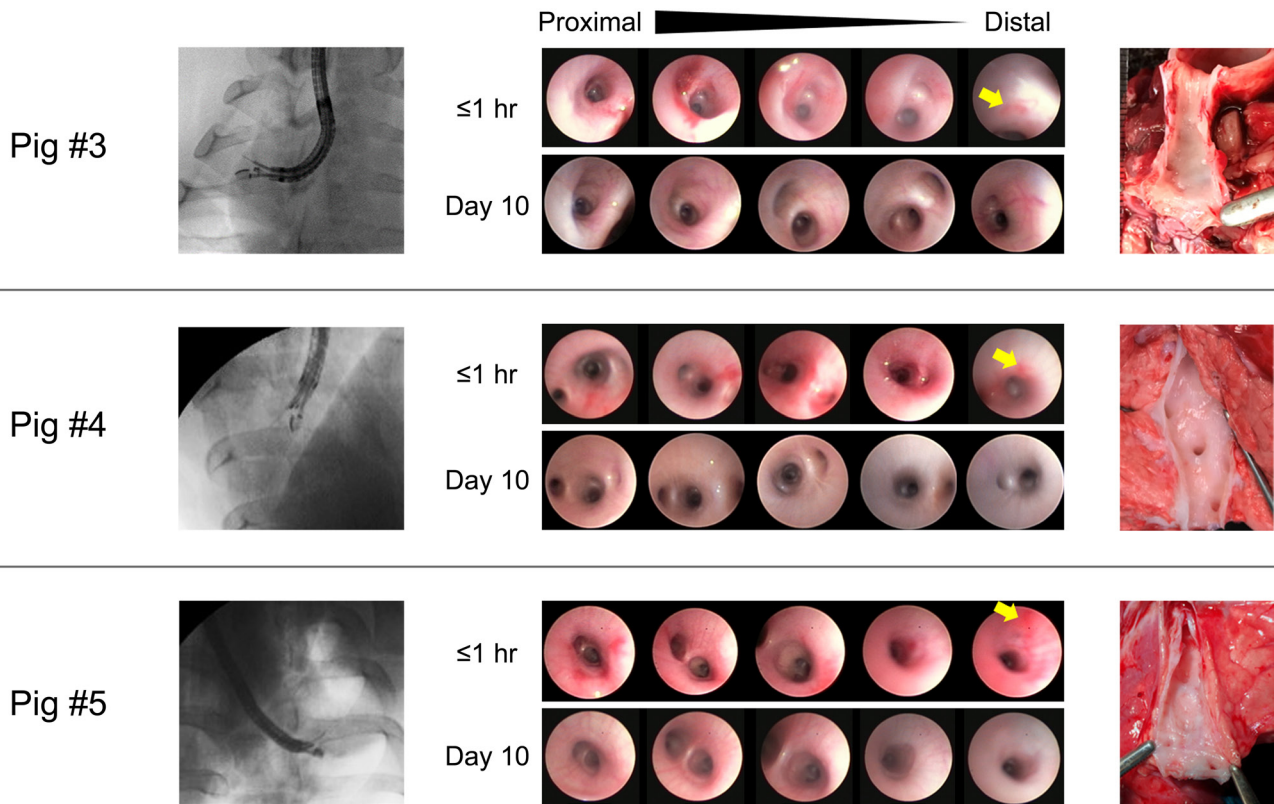
Figure S3 Medium-term safety of TCP-EBUS-guided TBNA in the peripheral lungs of live pigs, continued from *Figure 3*. Left, fluoroscopic images during TCP-EBUS-guided TBNA; middle, endobronchial findings at ≤1 h (top, yellow arrows indicate the needle insertion point) and at day 10 (bottom) post-TCP-EBUS-guided TBNA; right, gross pathology on day 10. TCP-EBUS was inserted into the right upper lobe in pig #3, the right lower lobe in pig #4, and the lingula in pig #5. In all pigs, erythema of the bronchial mucosa was observed right after insertion of the TCP-EBUS. However, the erythema self-resolved by day 10. All pigs showed normal respiratory status over the 10-day monitoring period. TCP-EBUS, thin convex probe endobronchial ultrasound; TBNA, transbronchial needle aspiration.

Figure S4 Cone-beam CT images of a representative case (Pig #2) 10 days after TCP-EBUS insertion into the distal airway. Yellow dots show the distal-most insertion point of the TCP-EBUS from Day 0, as confirmed by the endobronchial images. No abnormal infiltrates are observed in the lungs. CT, computed tomography; TCP-EBUS, thin convex probe endobronchial ultrasound.
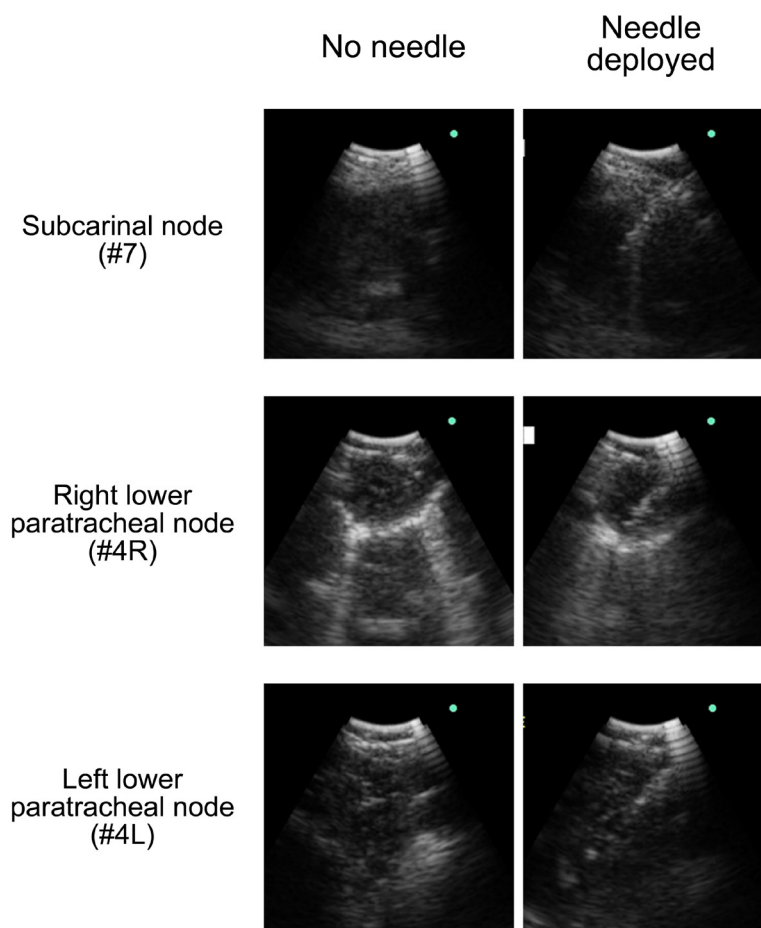
Figure S5 Representative ultrasound images of TCP-EBUS-guided TBNA of mediastinal lymph nodes in live pigs. The deployed 25-gauge needle is clearly seen on ultrasound within the lymph node without any impairment in visualization. TCP-EBUS, thin convex probe endobronchial ultrasound; TBNA, transbronchial needle aspiration.

Table S1 Subject characteristics and diagnostic outcome in *ex-vivo* assessment

Case	Age (y)	Gender	Lobe	Segment	Lung field	Lesion size (mm)	Radiographic lesion type	Bronchial generation	Bronchial diameter (mm)	Surgery type	*Ex-vivo* TCP-EBUS diagnosis	Final pathological diagnosis
#1	67	M	LUL	S4	Middle	21	Solid	3	4	Lobectomy	Ad	Ad
#2	72	M	RUL	S2	Middle	35	Solid	4	3.8	Lobectomy	Ad	Ad
#3	57	F	RML	S4	Middle	22	Solid	4	3.1	Lobectomy	Sm	Sm

The lesion size and the bronchial diameter were measured from the preoperative computed tomography images. Gender M, male; F, female; LUL, left upper lobe; RUL, right upper lobe; RML, right middle lobe; TCP-EBUS, thin convex-probe endobronchial ultrasound; Ad, adenocarcinoma; Sm, small cell lung cancer.